3. ATTENUATION OF THE VELOCITY WITH THE DISTANCE FROM THE POINT OF EXCITATION

3.1 Background

The classical bending-wave equation for vibrations of thin plates caused by harmonic point forces gives expressions for the transverse velocity (v) and the power transmitted to the structure by the force. This theory describes the velocity near the excitation point and in the free field at a distance due to the the propagating flexural waves. Additional velocities must be considered if the plate (or any structure) is thick and low-mobile.

A force acting on a small area (e.g. a machine footing) will give a local deformation that could be described as a Boussinesq-type displacement, see chapter 1 and section 2.4. The local point mobility (Y_{LOC}) was studied in the previous chapters for the purpose of determining if local power absorption affects power input measurements. Our conclusion is that this local absorption won't affect the average power input. The point mobility may be almost totally governed though by the local mobility in a typical concrete slab. Now, the aim is to understand how points on a concrete slab, typical in housing and industry, can be characterized with a point mobility (Y_0) and transfer mobilities.

First, the deformation in and around the excitation point is studied. The decay of the different waves is calculated, the velocity at a distance is divided into local/reactive, direct and diffuse field components. The aim is simply to understand how the point and its vicinity react to the force. In order to compare and to verify some of the conclusions, measurements were carried out, see [4.5].

Components of deformation

The deformation (d) as a function of the distance to the center of the excitation point (r) consists of several components, see section (2.4) and figure 2.4.

Attenuation of the direct field

The components of motion described in (2.4) change a lot outside the indenter. Only the bending wave component causes motion outside the area with the local deformation. The local deformation of the plate surface is assumed to follow eq. (3.1).

$$d = F \frac{(1 - \nu^2)}{\pi E a} \arcsin\left(\frac{a}{r}\right) \qquad (3.1)$$

The displacement at a distance 8a is only 8% of the maximal displacement, i.e. 20 dB smaller than that straight under the indenter. Thus, a measurement of the point mobility with force and velocity transducers separated underestimates Y_0 and also causes a phase-error that is not negligible, nor easy to compensate for (see 2.4) and figure 4.4. The near-field and the propagating bending wave fields, can be described with (eq. 2.10)

$$v(r) = v_0 \left(H_0^{(2)}(kr) - H_0^{(2)}(-jkr)\right) = v_0 \Pi(kr) \qquad (3.2)$$

which for $kr > 4$ can be replaced by the asymptotic expression: (eq. 2.11)

$$v(r) = v_0 \sqrt{\frac{2}{\pi kr}}\, e^{-j(kr - \pi/4)} \qquad (3.3)$$

With $0.8 < kr < 4$, the error in v(r) in the asymptotic expression (3.3) is less than 1 dB, but for $kr < 0.8$ the error increases rapidly so that the asymptotic expression exaggerates v. At a distance this direct field component may underestimate the velocity because a diffuse field is superimposed on the direct field. This is discussed in next part.

3.2 Direct and diffuse field "around" the point

The direct field velocity component, rms values denoted $v_{DIR}(kr)$ can be written as

$$v_{DIR}^2(kr) = \frac{P_{IN}}{\mathrm{Re} Z_0} \cdot \left|\Pi(kr)\right|^2$$

$$= \frac{P_{IN}}{8\sqrt{m'B'}} \cdot \left|\Pi(kr)\right|^2$$

which for $kr > 4$ can be approximated by

$$v^2_{DIR}(kr) = \frac{P_{IN}}{8\sqrt{m'' B^3}} \cdot \frac{2}{\pi kr} \qquad (3.4)$$

v^2_{DIR} is a function of both 1/r and $1/\sqrt{\omega}$.

For values of kr below 0.8, Hankel functions $H_0^{(2)}(kr)$ must be used, but the velocity doesn't increase very much from $v^2_{DIR}(kr = 0.8)$ towards the centre of excitation, for instance, $v^2_{DIR}(kr = 0.1)$ is only about 1.2 times higher. This is natural because of the flexural properties, the plate won't show a discontinuity at the point of excitation.

At some distance from the excitation point, the reverberant field will contribute significantly to the total velocity of the plate. If the bandwidth is big so that the reverberant field is diffuse, and if the power supply is fairly constant, a comparison can be made to achieve an expression that gives a velocity level in a remote point calculated from both the direct and the reverberant fields, in a quite similar manner as in room acoustics.

Assume that the power supply P_0 equals the total amount of power absorbed by the plate and that the plate has damping (η) and area (S). The direct field component of the velocity can be expressed by an intensity (instead of eq. [3.4]):

$$v^2_{DIR} = P_0/(2c_B \cdot 2\pi r \cdot m'') \qquad (3.5)$$

The power absorbed by the plate (P_{ABS}) can be calculated [2] as

$$v^2_{DIFF} = P_{ABS}/(\omega\eta m'' S) \qquad (3.6)$$

where v^2_{DIFF} is the spatial averaged velocity within a bandwidth $\Delta\omega$, that contains at least 5 modes and where $\omega/2\pi$ is the center frequency. The total velocity (v^2) consists of the direct- and the diffuse-field [8] added

$$v^2 = v^2_{DIR} + v^2_{DIFF} \qquad (3.7)$$

The cross-product $(2 \cdot v_{DIR} \cdot v_{DIFF})$ equals zero as the velocities are uncorrelated.

Transferred to levels, the velocity as a function of frequency and distance to the point of excitation is

$$L_v = L_{\underline{p}} + 10 \log \left(\frac{1}{2c_g + 2\pi r \cdot m''} + \frac{1}{\omega \cdot \eta \cdot m'' \cdot S} \right) \text{ for } kr > 0.8, kh < 1 \quad (3.8)$$

The term $(2c_g + 2\pi r \cdot m'')^{-1}$ corresponds to ϑ^2_{DIRECT}, the direct field, and $(\omega \cdot \eta \cdot m'' \cdot S)^{-1}$ corresponds to ϑ^2_{DIFF}, the diffuse or reverberant field. Together, they show the total velocity at unit power input, that is when $L_{\underline{p}} = 0$. (The local deformation is not included in eq. (3.8)).

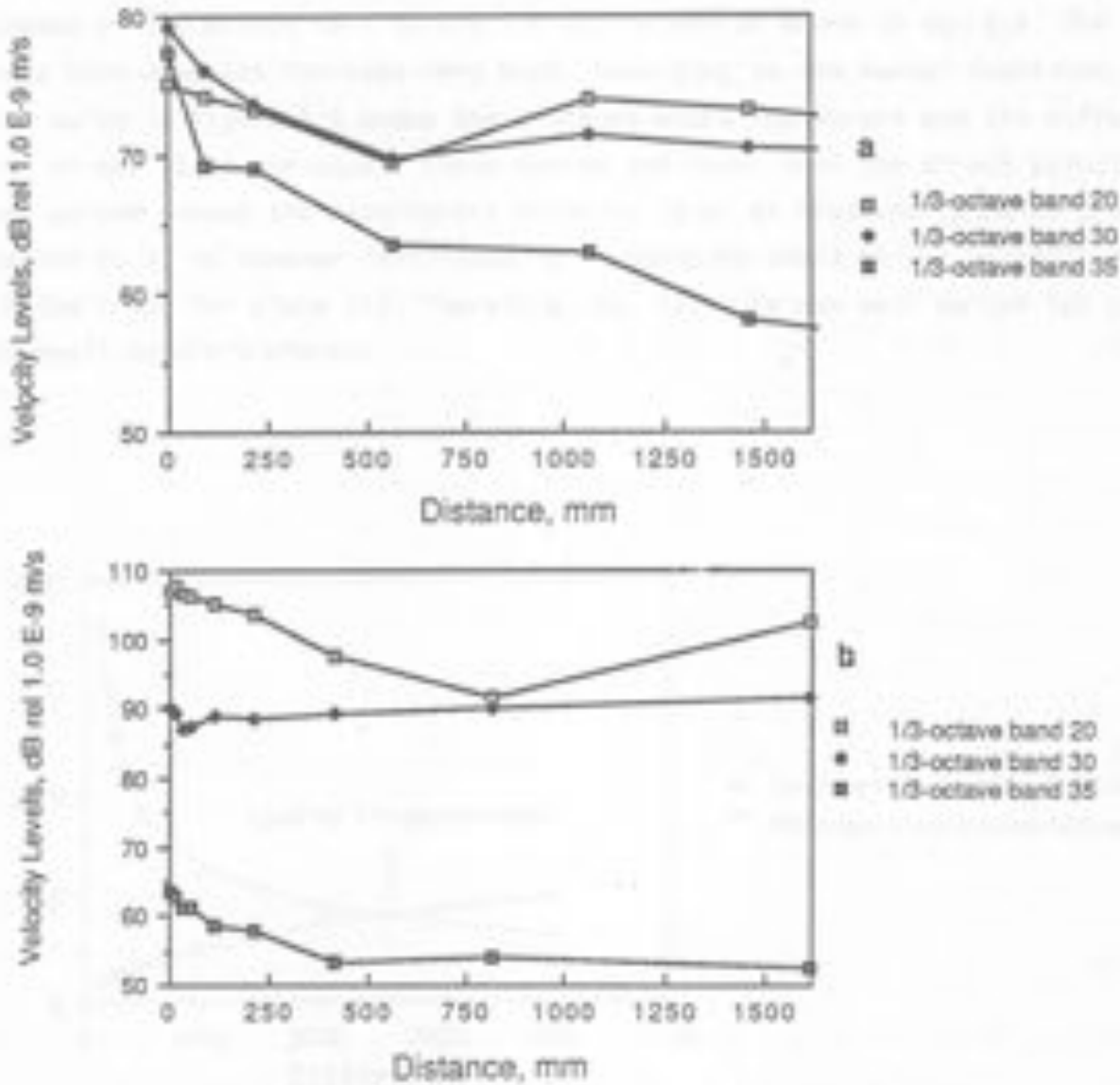

Figure 3.1 Measured velocity levels in third-octave bands.

a) Plate (1). The plate was excited close to the center of the plate. The measurement points were along a row parallel to an edge.

b) Plate (2). The plate was excited at a corner. The measurement points were along an edge.

(The third-octave bands 20, 30 and 35 correspond to center frequencies 100 Hz, 1000 Hz and 3150 Hz.)

Measurements on two concrete plates (see (1.1), plate (1) and (2)) are shown in figure 3.1. The local deformation closer to the FDI than about 0.100 m explains the increasing velocity level at small distances. There is also a weak decrease at greater distances.

The range of validity of eq. (3.8), kr > 0.8 and kh < 1, corresponds in the case of the thicker plate (plate (1), h = 0.16 m) to

$$k < 6 \quad \text{and} \quad r > 0.13 \text{ m}$$

One of the curves in figure 3.2 shows the distance r at various frequencies that corresponds to the condition kr = 0.8. Smaller values of r do not give an increase of the direct term as the 1/r-approximation shows in eq. 3.8. The direct term does not increase very much, according to the Hankel-functions. The other curve in figure 3.2 shows the distance where the direct and the diffuse terms of eq. (3.8) are equal. These curves indicate, that the direct velocity level cannot exceed the reverberant velocity level at frequencies below 2-3 kHz. Equation (3.8) is however restricted to frequencies where kh < 1 as well, that is below 1 kHz for plate (1). Therefore, eq. (3.8) is not well suited for cases with small concrete plates.

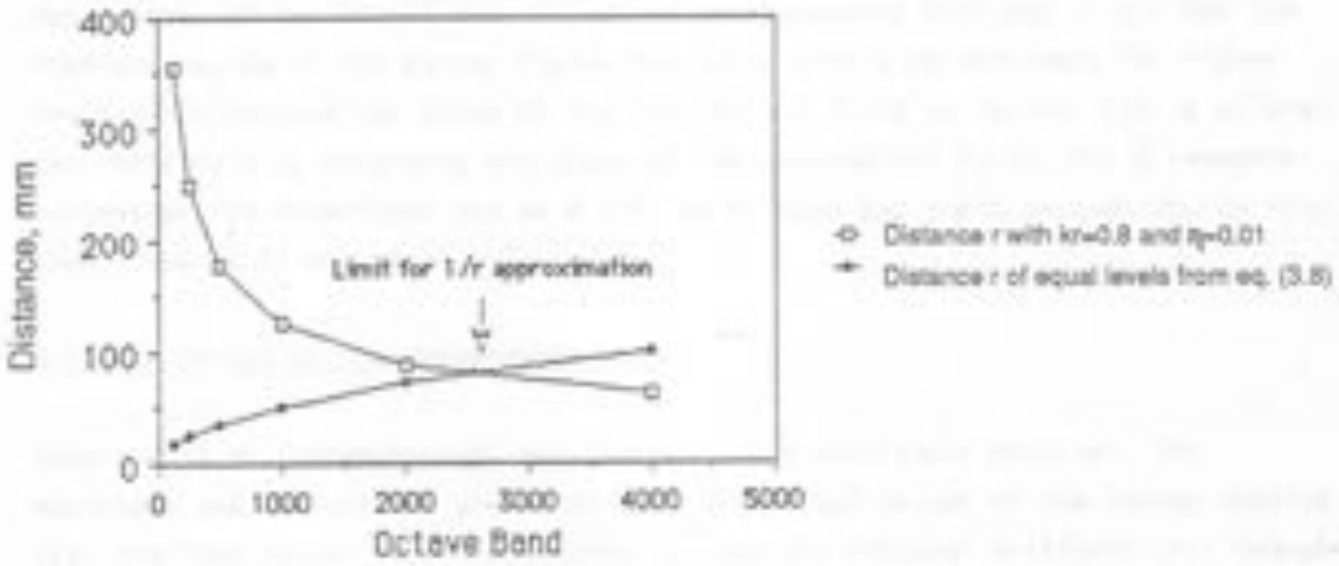

Figure 3.2. Lower curve (dark dots) shows the distance (r), where the diffuse and direct velocity terms are equal. The upper curve (boxes) shows the distance r with kr = 0.8, which indicates the region of maximum velocity close to the point of excitation. The "limit of 1/r approximation" arrow points out that equation (3.8) is not applicable below 2.5 kHz in our case, plate (1).

The aim was to derive an expression that gives the extension of the direct field on a plate around the point of excitation. The equation (3.8) doesn't work on small, lightly damped concrete plates however. Therefore, one is forced to use the more general expression (2.10a) to understand how the direct field decays with increasing distance. Unfortunately, this expression is difficult to interpret in this context. If the velocity is computed within a bandwidth and with many modes excited, the product of the two mode functions is always positive at the point of excitation (x_0,z_0), and the sum is therefore in the average greater than the sum of the products of the mode functions at the point of excitation and another point

$$\sum_n \phi^2_n(x_0,z_0) \leq \sum_n \phi_n(x,z)\phi(x_0,z_0)$$

$$v(x_0,z_0) > v(x,z)$$

It is however difficult to calculate how far the direct field extends. To study this phenomenon in detail, transfer mobility measurements were carried out. The remote velocities normalized with respect to the excitation point velocity were measured as transfer and point mobilities divided. The results are presented and interpreted in section (4.5). They show that the velocity in the remote point is governed by the direct field (see eq. (3.4)) for low frequencies but above a certain frequency, the field becomes diffuse. The phase also supports this observation of the magnitudes, it varies approximately with exp (- kr) for low frequencies, as in the direct field, but falls with a certain rate for higher frequencies because the phase of the reverberant field is random. (It is at present difficult to interpret the phase of the reverberant field, but a research project at the department and at M.I.T. by R. Lyon may yield methodology in this area.) See (4.5) and (4.4).

3.3. The choice of the measurement point

Concrete is an inhomogeneous, non-isotropic and non-linear material. The equations and evaluations are often used with fixed values of the Youngs modulus (E), the loss factor (η), the density (ρ) and the flexural stiffness (B), though they could vary within the same plate as well as from one plate to another. Results from one particular structure may not apply in a case that could look similar at a glance. Measurements on a specific concrete structure may yield results that could not be generalized and used in a prediction situation. Although those difficulties are important, there is no choice but to assume certain properties in order to enable any evaluations at all. There was, and still

is, a need for experience of measurements on concrete structures, especially since it is a very frequent building material. However, to see how the choice of a point on a concrete slab (with dimensions typical in housing) affects the measured value of the point mobility, several measurements have been made.

It is possible to derive an expression for the point mobility of finite plates, from two different points of view. One is wave-analytical and derives the point mobility by considering only waves radiated outward by driving an infinite plate at one point. The other derivation averages over modes of a finite plate and presumes that waves reflected at the boundaries don't affect the point mobility because they will have a random phase [8]. According to the theory for the point mobility of an infinite plate, Y_0 is real apart from the influence of the local deformation.

The number of modes (N), within a bandwidth Δf, is of importance when statistical models are employed as in (2.3) and (2.4) where spatial averages are employed. The eigenfrequencies are essential in measurement evaluations. The number of modes per frequency unit [2] for the bending waves is

$$\frac{\Delta N}{\Delta f} = 2\pi \cdot \frac{S}{4\pi} \cdot \sqrt{\frac{m''}{B'}} = \frac{S}{2}\sqrt{\frac{m''}{B'}} \qquad (3.9)$$

Applied on a concrete slab with $S = 11.7\ m^2$ and $h = 0.16\ m$, $\Delta N/\Delta f$ is

$$\frac{\Delta N}{\Delta f} = 0.037$$

and $N\ (f < f_{max}) = \frac{\Delta N}{\Delta f} \cdot f_{max} = 0.037 \cdot f$

The eigenfrequencies (f_n) for a simply supported plate can be calculated from the plate dimensions [2] as

$$f_n = \frac{1}{2\pi} \cdot \sqrt{\frac{B'}{m'}} \cdot \left(\left(\frac{n_1 \cdot \pi}{l_1}\right)^2 + \left(\frac{n_2 \cdot \pi}{l_2}\right)^2\right) \qquad (3.10)$$

The concrete slab (Plate (1)) used as an example has some 9 eigenfrequencies below 300 Hz, the first is at 45 Hz. The condition "at least 5 modes within the bandwidth" means that the bandwidth must be greater than 150 Hz in the analysis.

Measurements were made in five different locations on a plate. The distance between adjacent locations was typically half the indenter radius. An annular indenter (the FDI) with the velocity transducer mounted in the cavity of the indenter was used. The worst case of inhoeogenity would be a cavity in the concrete next to grains or gravel with high stiffness and diaensions in the order of the size of the FDI. It would cause rotation of the indenter and a change in the local compliance. The results are discussed in (4.6).

3.4. Transfer mobility measurements

Introduction

The power transmitted through a coupling point, from the source through a footing or a vibration isolator, into the structure has been treated as if there is only one contact point. The power transmitted is

$$P_{IN} = \frac{1}{2} \mathrm{Re}\,[F \cdot v^*] = F^2 \cdot \mathrm{Re}\,(Y_0) \qquad (3.11)$$

When a multi-point system with coupled points is studied, the power transmitted can be calculated with a similar expression. The total amount of power transmitted to the receiving structure through N contact points can be calculated as

$$P_{IN} = \sum_1^N P_n, \qquad (3.12)$$

where the power transmitted through one of the points (P_n) is computed as a product of the squared force acting in the point (F_n) and an effective mobility (Y_{eff}) that replaces Y_0 in the expression above. Y_{eff} is a sum of transfer mobilities of all points and the ordinary point mobility (Y_0) [1]:

$$Y_{n,eff} = (\sum_{k=1}^N (Y_{kn} \cdot F_k))/F_n \qquad (3.13)$$

The power transmitted through one of the points, with the interaction between the points included:

$$P_n = F^2 \mathrm{Re}\,[Y_{n,eff}] \qquad (3.14)$$

and the total power transmitted to the structure is simply a sum of P_n from all points [1]. Now, as Y_{eff} includes transfer mobilities, it is of interest to study how the transfer mobility (Y_{kn}) is influenced by the local deformation on low-mobile structures. Several kinds of installations, constituting vibrational sources of great importance, are multipoint installations on low-mobile structures. The distance between the contact points may be short enough to give a high degree of coupling between the points. The power transmitted must be calculated with effective mobilities.

To study the dependence of the transfer mobility with the distance, and to compare it with the ordinary point mobility as a function of frequency, measurements were made.

In figures 4.6 and 4.7, $|Y_{Dr}|$ and the phase (Y_{Dr}) are presented as the normalized functions $|Y_{Dr}| / |Y_D|$ and respectively, phase (Y_{Dr}) - phase (Y_D). Those graphs contain a lot of information, they tell something about how the local deformation decays with the distance and for which kr the direct field becomes less than the diffuse field, as discussed in (3.4). See (4.5).

4. RESULTS AND INTERPRETATIONS

4.1. Measurements of driving power supply and power absorbed by the plate

Measurements were made of the spatial averaged velocity according to (2.3) in order to compare the power absorbed by the plate with the measured power input. The narrow-band measured input power, proportional to Re Y_0, required an amount of programming and consideration to be summed to values for each $\Delta\omega$. Furthermore, a great number of measurements of the quantities Re Y_0, $\bar{F}^2$, η and $\langle \dot{v}^2 \rangle$ were made, to yield a maximum of precision in the difference between the input power and the power absorbed. As a matter of fact, it was found extreeely difficult to obtain reasonable precision in the difference $P_{IN} - P_{ABS}$. Therefore it was not judged meaningful to present the results in the report. There are too many difficulties inherent in the measurement method, e.g. to interpret the decay curves to get η.

4.2. Measurements of Re Y_0 with different indenters

The description of the measurement is in (2.2). Results and interpretations are presented in this section. See figures 4.1 and 4.2.

Some results

Re Y_0 increases with the frequency in all measurements - most pronounced at higher frequencies.

Re Y_0 varies with the frequency and with the size of the indenter, but the influence of the size cannot be evaluated from these measurements. If various measurements are made on different objects, an ensemble average of all measurements may yield a clear tendency in the variation of Re Y_0 with the indenter size.

Re Y_0 averaged over several modes, is close to $Y_\infty = 1/8 \sqrt{m'' B} = 2 \cdot 10^{-6}$(m/sN) at frequencies below kh = 1 (about 1 kHz). Compare with section (4.3) and figure (2.2).

Interpretations of increasing realpart

The real part of the point mobility increases with the frequency, as can be studied in figures 4.1 and 4.2. This phenomenon doesn't fit the classical

theoretical predictions of the point mobility, but can be attributed to several possible physical reasons, which are discussed here.

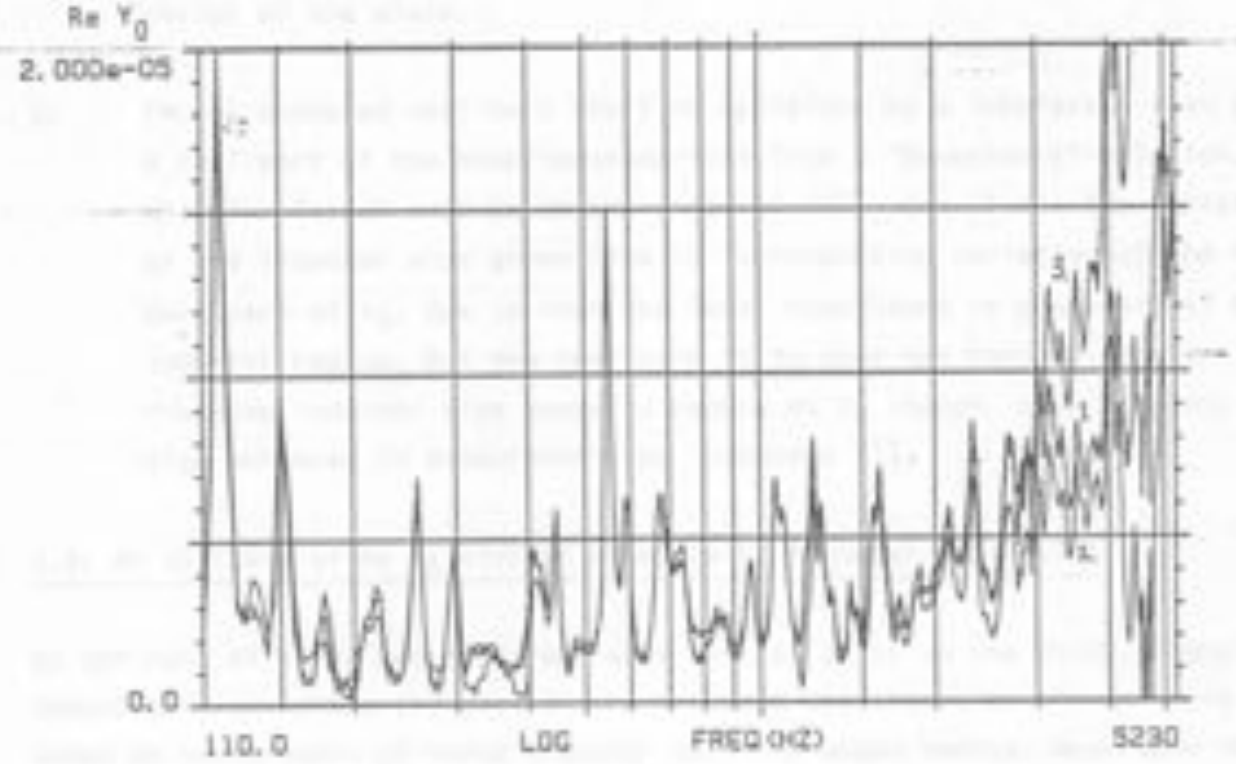

Figure 4.1. Re Y_0 for 3 indenters: centre of the plate. (plate 1)
1. $a = 25 \cdot 10^{-3}$ m 2. $a = 50 \cdot 10^{-3}$ m 3. $a = 75 \cdot 10^{-3}$ m.

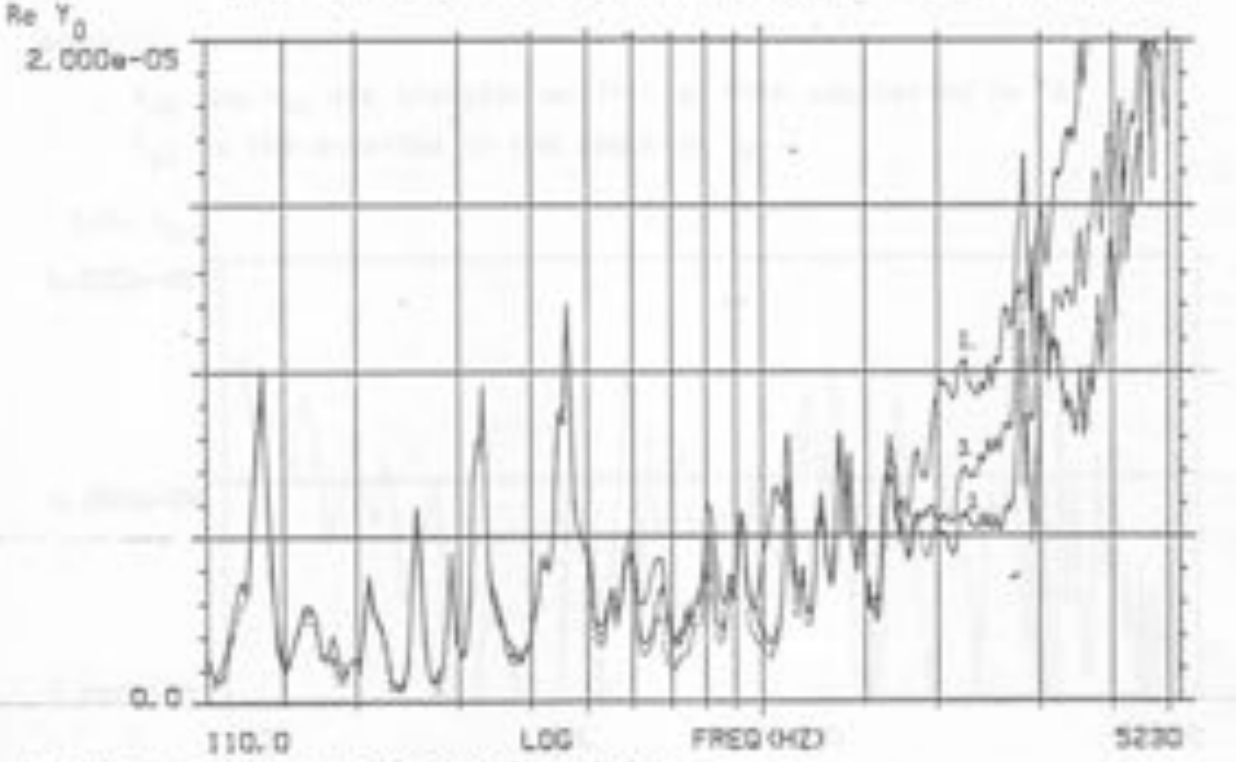

Figure 4.2. Re Y_0: non-central position.
Legend - see figure 4.1.

1) When the excitation frequency rises above the frequency corresponding to kh = 1, (here = 1 kHz), shear deformation will increase the mobility significantly. P_{IN} also increases due to power input into shear deformation of the plate.

2) If the measured real part shall be explained by a lossfactor that gives a real-part of the compliance derived from a "Boussinesq"-solution, then this lossfactor must be in the order of 10^{-1}. See (2.2). The variation of the indenter size gives rise to corresponding variation of the imaginary part of Y_D, due to that the local compliance is proportional to the indenter radius. But the real part of Y_D does not vary as regular. An increasing indenter size seems to reduce Re Y_D though, that tendency is also achieved in measurements by Petersson [1].

4.3. An estimate of Re Y_D with an envelope of transfer mobilities

An estimate of Re Y_D was performed at a central point on the thick, lightly damped concrete plate (1) used in the previous measurements. The estimate is based on measurement of three transfer mobility measurements, described in section (2.5), eq. (2.16).

$$E\,[\mathrm{Re}\ Y_D] = |Y_{AB}| \cdot |Y_{AC}|/\hat{Y}_{BC} \qquad (4.2)$$

where

Y_{AB} and Y_{AC} are transfer mobilities with excitation in "A"

$\hat{Y}_{BC}$ is the envelope to the peaks in Y_{BC}.

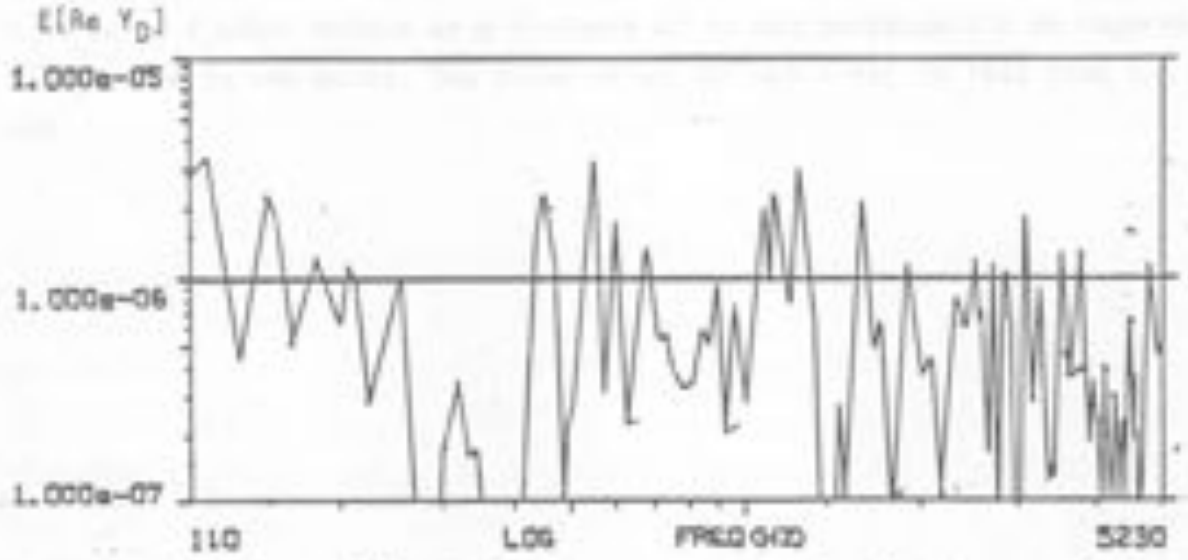

Figure 4.3. Re Y_D, calculated from measurements according to eq. (4.2).

The envelope on $\hat{Y}_{BC}$ was made by hand, but can be automated. It is probably easier to add several estimates though. Re Y_D, calculated from eq. (4.2), is less than the estimates E [Re Y_0] in section 4.2 show. The shape of the curves is very similar, peaks and anti-resonances fit, which at least indicates that the method described in section (2.5) gives an estimate of Re Y_D. The difference in magnitude could be related to

- local dissipation of power, i.e. Re Y_D < Re Y_0
- other physical reasons or measurement errors.

The measurement yielded a difference in magnitude, but the conclusion is at present that the method is not sufficiently verified.

4.4. Estimation of the local mobility through transfer mobility measurements

4.4a). Measurements beside the indenter

In sections (3.1) and (2.4) fig 2.3, the deformation of the plate surface from the pressure of the indenter was assumed to obey an arcsine curve. Figures 4.4a) and b) show the magnitude and the phase of the point mobility (Y_0) and a spatial averaged transfer mobility (Y_{0r}) at a certain radius r. Y_{0r} is called Y_{20} in the discussion in section 2.4. (Four averages were made around the point). The radius was chosen to be close enough to "avoid" attenuation from propagation but also distant enough to suppress the influence of the local deformation.

At the distance 8a (0.096 m), the calculated attenuation of the local deformation is 18 dB and that due to propagation is less than 5 dB (below 5 kHz, only 2 dB below 2 kHz). Points at a distance of 8a may consequently be regarded as being close to the point. The phase delay (kr = k · 8a) is less than 1.4 below 5 kHz.

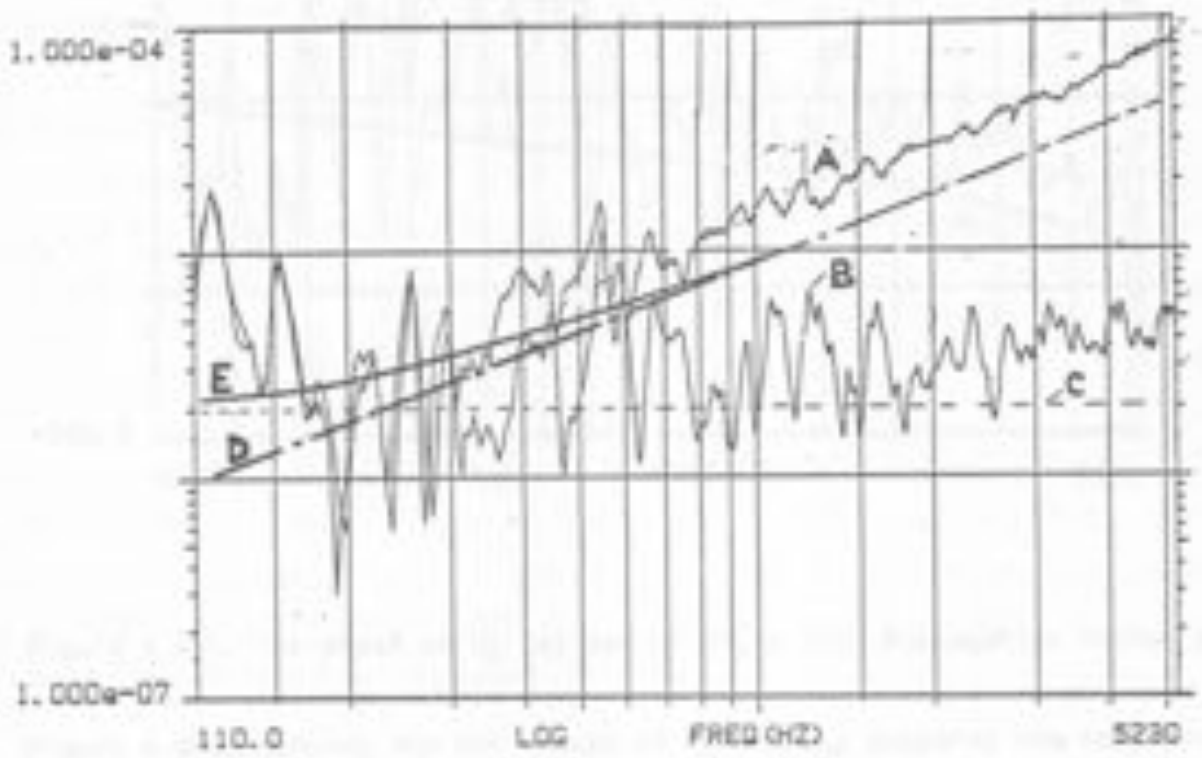

Figure 4.4a) Calculated and measured Y_i:

A. Measured Y_0

B. Measured $\langle Y_{0r} \rangle$, r = 0.1 m, 4 averages

C. $Y_\infty = 1/8 \sqrt{\pi^{-1} S^{-1}}$ from eq. (2.7)

D. ωC from eq. (2.2b)

E. $Y_\infty + j\omega C$

Figures 4.4a) and b) show that the measured Y_0 increases with 6 dB per octave and that the phase is close to 90° above 0.5 kHz, which proves that the local compliance governs the point mobility. Y_{0r} is close to Y_0 for low frequencies were both kr and ωC are small, and doesn't increase with the frequency as is predicted. The resonance pattern is similar to that of Y_0 but is more pronounced.

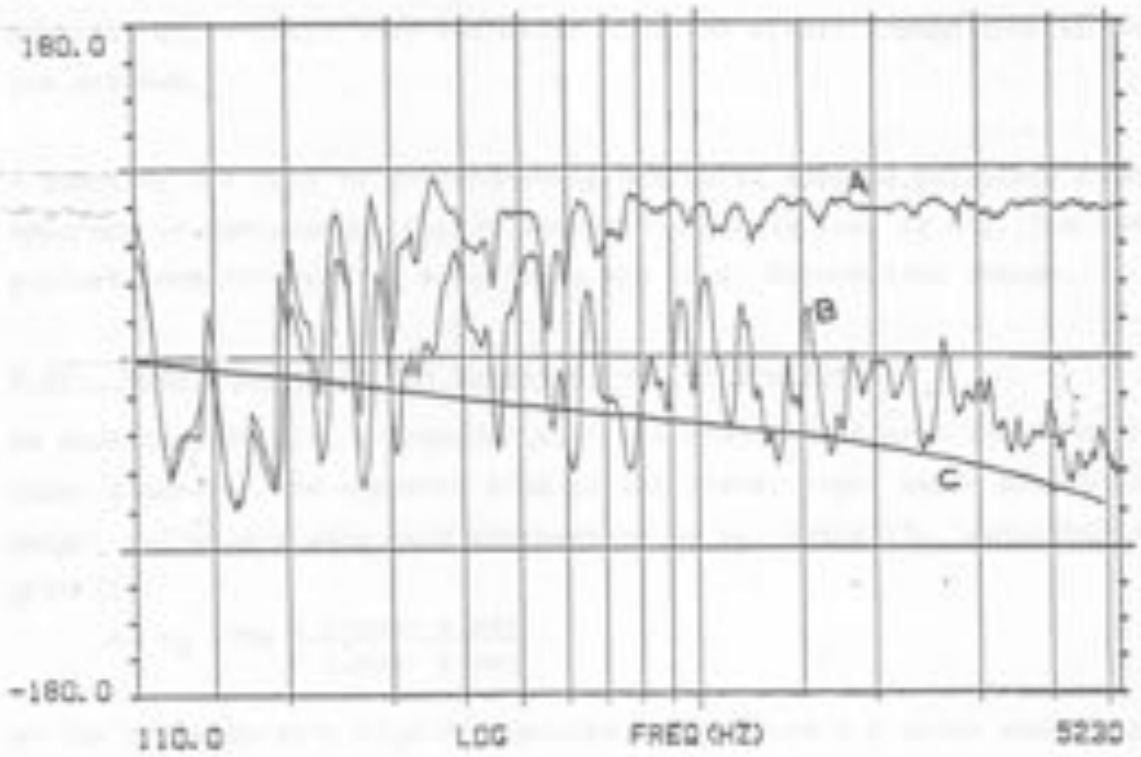

Figure 4.4b). The phase of Y_Q (A) and of $\langle Y_{Qr} \rangle$ (B). Propagation factor e^{-jkr} (C).

Figure 4.4b), showing the two phases of Y_Q and Y_{Qr} supports the conclusions although the phase (Y_{Qr}) decreases with the frequency due to the propagation delay (e^{-jkr}). (The phase accuracy below 400 Hz is reduced due to weak coherence. This affects mainly at resonances and antiresonances, the tendency though is correct).

The magnitudes of Y_{Qr} were compared to a theoretical value of the point mobility for an infinite plate (Y_∞) which is real, and a complex mobility with Y_∞ as the real part and $j\omega C$ as the imaginary part. For comparison, see "C - E" in figure 4.4a). For low frequencies, they fit rather well but for higher frequencies, a discrepancy in the order of 4 - 6 dB arise. It may be referred to at least three reasons:

the effective radius (area) of the indenter is less than assumed (= a)

the Youngs Modulus (E) is less than assumed

losses occur in the point of excitation so that Y_{LOC} is complex and consequently greater than the reactive local mobility part ($j\omega C$).

The discrepancy is about the same in Y_{Dr} and Y_D when compared to the fictive mobility ($Y_m + j\omega C$). That indicates that the actual Youngs modulus differs from the assumed.

A quantity (Re Y_{Dr}) is unfortunately not quite easy to calculate since the phase accuracy is not enough, due to propagation delay (see (2.4)). The measurements yielded some interesting aspects on the local deformation though.

4.4b). Measurements on the opposite side of the plate

As described in 2.4, a transfer mobility measurement with the velocity transducer placed on the opposite side of the plate, right under the force transducer, can give a very good estimate of Re Y_D. Actuallly, according to Ljunggren [9].

$$\text{Re } Y_D = \text{Re } \frac{v \text{ (lower side)}}{F \text{ (upper side)}}$$

at low and moderatly high frequencies. See figure 4.5 which shows the real part of the transfer mobility and of the point mobility. The measurement object was plate (2). As can be seen in the figures, the curves are almost identical. This approach indeed indicates that practically no local absorption of power occurs since the differences are small.

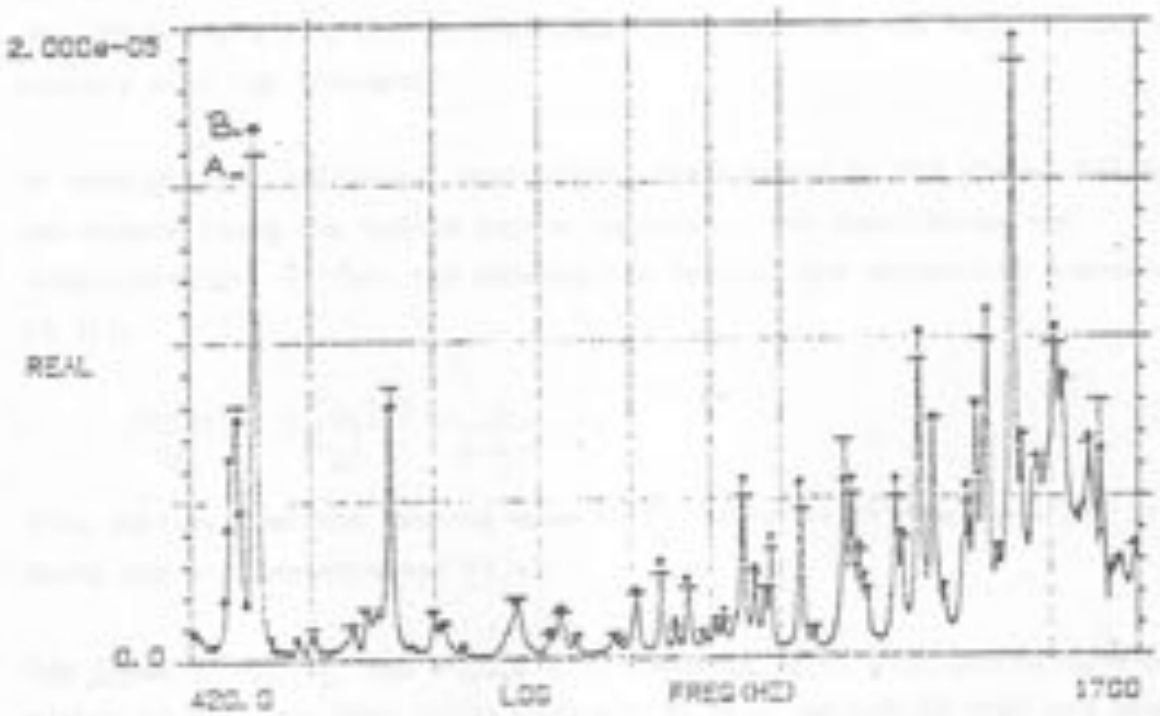

Figur 4.5. Real parts of point and transfer mobilities on plate (2).
(A) shows the real part of the point mobility.
(B) shows the real part of the transfer mobility, where the excitation is identical that of (A) and the velocity is measured on the opposite side of the plate 420 - 1700 Hz.

4.5 Interpretations of transfer mobilities - direct and diffuse fields

Figure 4.6 shows transfer mobilities at a distance (r), normalized with respect to Y_0. They give information about the decay of the local deformation. Coming closer to the point than 100 mm, as in previous discussion, is shown in figure 4.6. The calculated attenuation of C in section (3.3) is compared to a few transfer mobilities at certain distances, C(r)/C. One can hardly conclude that the curves fit an arcsine curve exactly, but the tendency shows that the assumption (from 3.3), that the statical displacement of a half-space may be extended to a thick plate in the high frequency domain, seems to apply rather well. For greater distances, they also tell something about the relationship between the direct - and the diffuse - field behaviour. Furthermore, they enable an interpretation of the importance of the transfer mobilities in the context of effective mobilities (see (3.6)).

The normalized transfer mobilities (Y_{0r}/Y_0) in the figures 4.6 and 4.7 must be interpreted with respect to both the distance and the frequency.

At small distances, as discussed in section 4.4, the attenuation with r is primarily caused by the decay of the local deformation with r. A direct field is measured because the attenuation due to propagation is small. At greater distances, from $r = 0.2$ to 0.7 m, the tendency is obvious, the velocity decreases rapidly with the frequency.

At even greater distances, approaching the borders of the plate, the spatial variations along the radius become important, and complicates the interpretation. As far, the attenuation follows the asymptotic expression (see (3.3)):

$$\left|\frac{v(r)}{v_0}\right|^2 = \left[\frac{|Y_{0r}|}{|Y_0|}\right]^2 = \frac{2}{\pi \cdot k \cdot r}$$

This implies that the bending wave field, which is diffuse does not affect the point mobility measurement at all.

The phase of Y_{0r}/Y_0, see figure 4.7, seems to decay with approximately $e^{-j(kr)}$ within $kr = 3$, but then falls with a high rate indicating that one measures in a diffuse field where the phase is random. This is contradictory to what is predicted in (3.4) from the power model, but not from a modal superposition point of view (eq. 2.10 a).

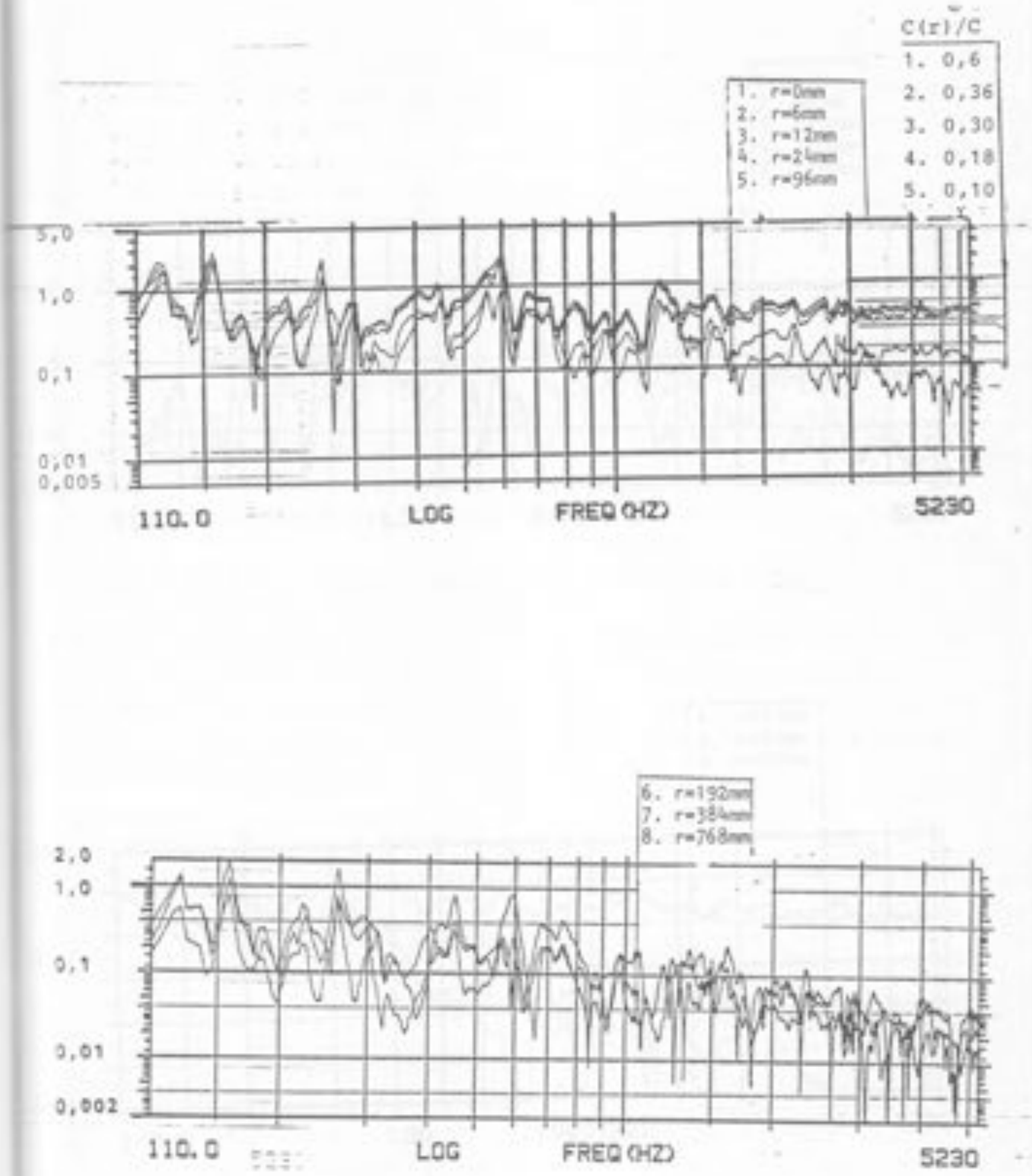

Figure 4.6. $|Y_{Qr}|/|Y_Q|$ with different values of r. The column C(r)/C refers to the decay of C(r), from eq. (2.13), for comparison. Above: $0 \leq r \leq 96$ mm, below $96 < r \leq 768$ mm.

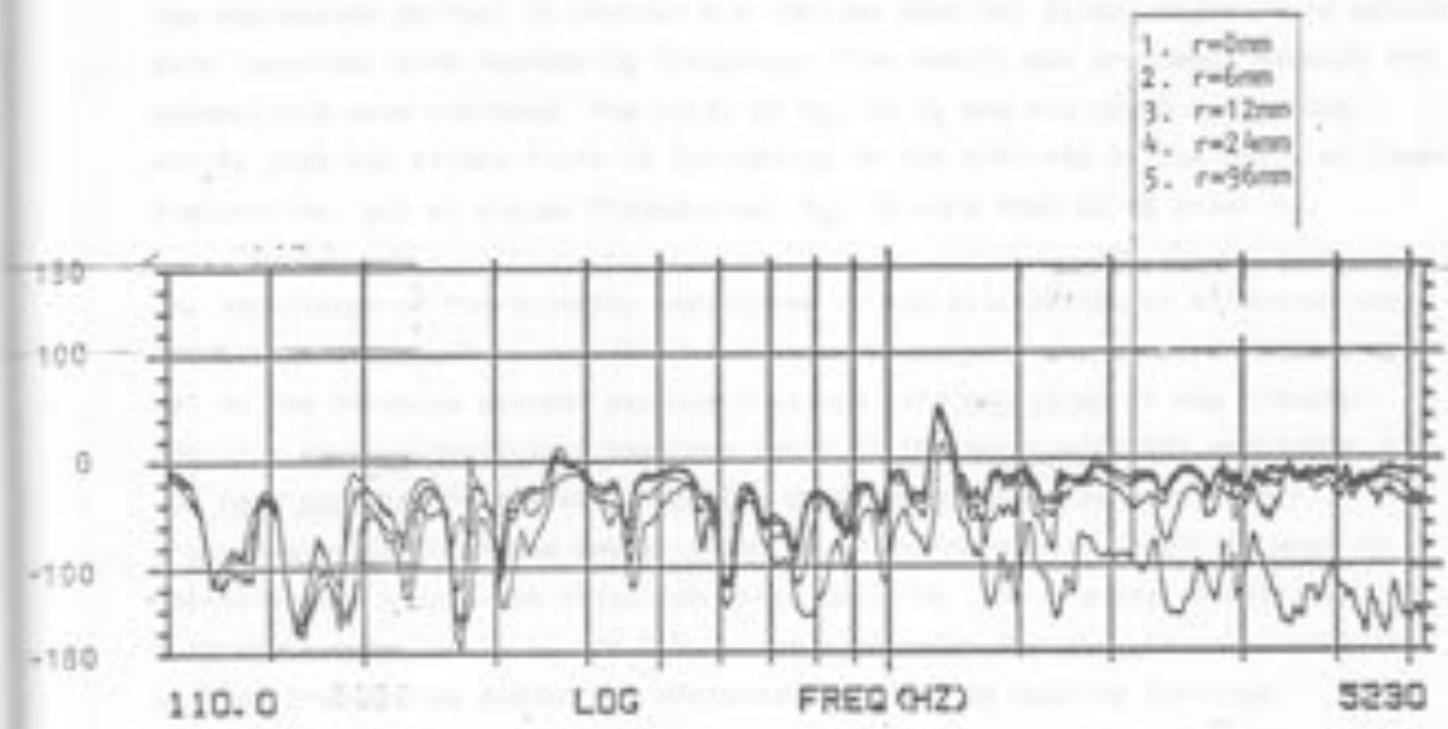

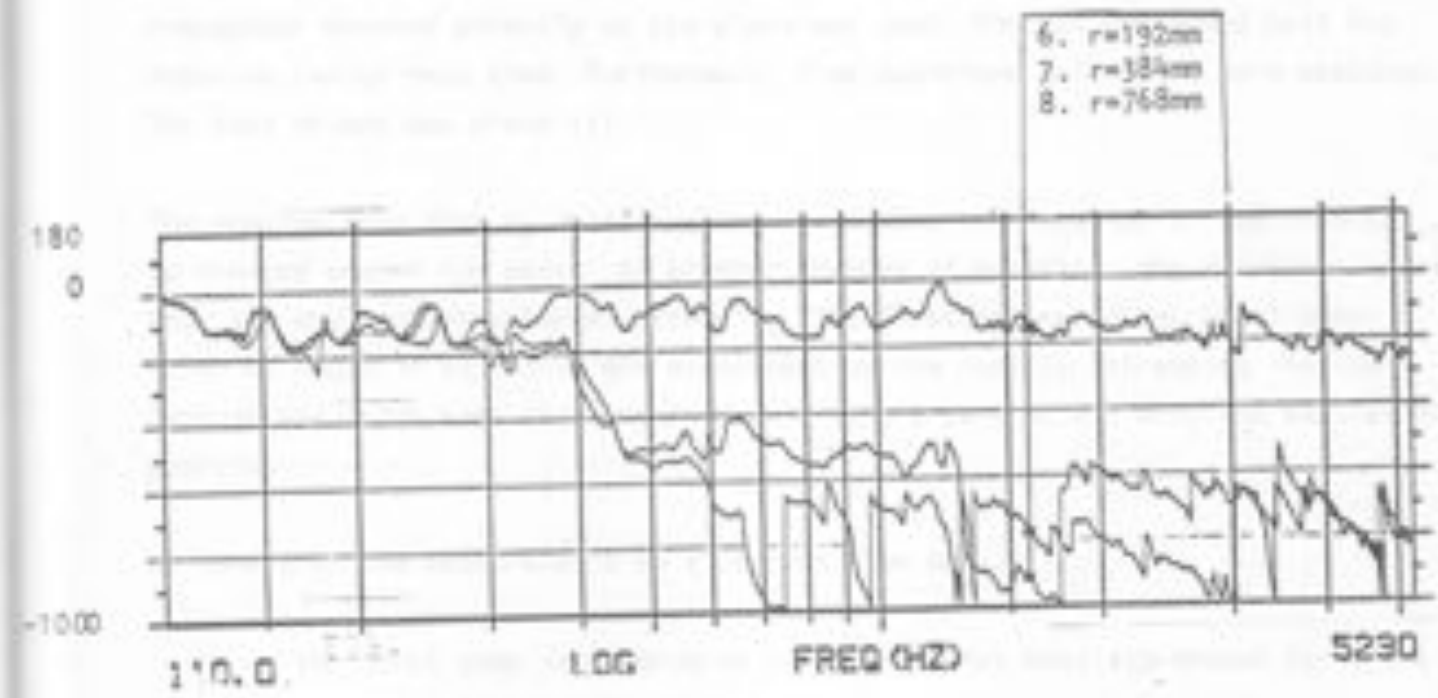

Figure 4.7. The phase difference (phase Y_{0r} - phase Y_0).

The expression derived in chapter 3.4 implies that the direct field would become more important with increasing frequency. This result was erroneous because the assumptions were violated. The ratio of Y_{Qr} to Y_Q and the phase difference verify that the direct field is dominating in the vicinity of the point at lower frequencies, but at higher frequencies, Y_{Qr} is more than 20 dB under Y_Q.

The importance of the transfer mobilities in the calculation of effective mobilities, as discussed in chapter 3.5: It can be concluded that at distances typical to the distance between machine footings, the magnitude of the transfer mobility is in general less than one tenth of the point mobility magnitude, but the real part of the transfer mobility does not decrease as much. Power transmission calculations may be based on an ordinary point mobility when it approximately equals the effective point mobility. The transfer mobilities contribute very little to the sum in the expression for the effective mobility at high frequencies and/or big distances between the machine footings.

4.6. Variations in Y_Q due to changes in the position of excitation

According to the discussion in [3.5], measurements were made with small variations around a point. An annular indenter (the FDI) with the velocity transducer mounted directly on the plate was used. The FDI was moved half the indenter radius each time. Furthermore, five positions well apart were measured. The test object was plate (1).

The results show that Y_Q doesn't change much when the location of the indenter is changed around the point. At greater changes of position, the different modes that are excited below 300 Hz affect Y_Q. The fluctuations due to modal behaviour at higher frequencies are suppressed by the rapidly increasing imaginary part of the point mobility, which doesn't hardly vary at all with the excitation position.

We interpret the measurements on a concret slab as

- the local compliance governs the total point mobility except for a few resonance frequencies below 1 kHz.

- The force and the velocity transducers must not be placed apart in a point mobility measurement. The size of an indenter affects the local compliance and thus the point mobility.

- The location of a point mobility measurement on the "inner" part of a plate doesn't affect the tendency of the mobility, a few spatial averages from different points even out the influence of resonances at a single point.

- An indenter (e.g. 25 mm diameter) seems to even out the influence of inhomogenities in the concrete under the indenter rather efficiently - hardly no variations at all could be detected. The indenter must be attached to a smooth surface, and glue or rubbing is advised to obtain a rigid contact. Impedance heads cannot be used at all, partly because of the soft force transducer that "isolates" the velocity transducer, partly because of the small contact area.

REFERENCES

[1] Petersson B. Studies of ordinary and effective mobilities for the determination of structure-borne sound power transmission. Doctorial Thesis, Dept of Building Acoustics, Chalmers University of Technology, Gothenburg 1983.

[2] Cremer L., Heckl M., Ungar E.E. Structure-Borne Sound. Springer Verlag, Berlin 1973.

[3] Kihlman T. Grundläggande teknisk akustik. Göteborg 1982.

[4] Hall J.R., Richart F.E., Woods R.D. Vibrations of Soils and Foundations. Prentice-Hall 1970. Englewood Cliffs, N.J.

[5] Pinnington R.J. Using the Envelope of Resonance Peaks to Estimate Power Absorbed by a Finite Structure. I.S.V.R. Techn. Report 115, 1981.

[6] Ljunggren S. Rapporter KTH 1986:1. (in Swedish)

[7] Ljunggren S. Acustica May 1986.

[8] Lyon R.H. Statistical Energy Analysis of Dynamical Systems. The MIT Press, Cambridge, Massachusetts.

[9] Ljunggren S. Free and forced Vibrations of Infinite Plates. Report S-3625-A. Ingemansson Acoustics. Stockholm.

[10] Jacobsen, F. Measurement of structural loss factors by the power input method. The Acoustics Laboratory. Rep. 41 1986.

[11] Ranky, M.F. et al. Frequency average loss factors of plates and shells. J.S.V. Vol 89 (3) 1983 p. 309.

[12] Adams, R.D. et al. Errors in Mechanical Impedance data obtained with Impedance Heads. J.S.V. Vol 73 (3) 1980 p. 461.

SYMBOLS

P	= power [W]
F	= force [N]
v	= velocity [m/s]
Y	= mobility $[\frac{m}{s \cdot N}]$
Z	= iepedance $[\frac{s \cdot N}{m}]$
ϕ	= diameter of indenter [m]
a	= radius of indenter [m]
r	= distance between center of indenter and a point [m]
d	= displaceeent
f	= frequency [Hz]
ω	= angular velocity, $\omega = 2\pi f$ [1/s]
k	= wave number for bending wave [1/m]
Π	= sum of two Hankel functions
B	= flexibility for a plate [Nm]
B'	= flexibility for a plate, per unit width
E	= Youngs modulus [N/m²]
ν	= Poissons ratio [1]
ρ	= density for concrete [kg/m³]
M	= $\rho \cdot S \cdot h$ = mass of the plate [kg]
m''	= $\rho \cdot h$ = mass per unit area [kg/m²]
h	= thickness of a plate [m]
S	= area of the plate [m²]
b, l	= width and length of the plate [m]
Re (), Im ()	= real and imaginary part of ()
K	= stiffness
C	= compliance
R	= resistance
$1/R$	= conductance
$E[x]$	= estimate of value [x]
L_x	= level, i.e. 20 log x rel 1.0 $\frac{m}{s \cdot N}$